

Composition dependent dynamics of biexciton localization in $\text{Al}_x\text{Ga}_{1-x}\text{N}$ mixed crystalsDaisuke Hirano,¹ Takeshi Tayagaki,¹ Yoichi Yamada,² and Yoshihiko Kanemitsu^{1,3,*}¹*Institute for Chemical Research, Kyoto University, Uji, Kyoto 611-0011, Japan*²*Department of Electrical and Electronic Engineering, Yamaguchi University, Ube, Yamaguchi 755-8611, Japan*³*Photonics and Electronics Science and Engineering Center, Kyoto University, Kyoto 615-8510, Japan*

(Received 22 July 2009; published 20 August 2009)

We report the localization-dependent dynamics of biexcitons in $\text{Al}_x\text{Ga}_{1-x}\text{N}$ mixed crystals under exciton resonant excitation at low temperatures. After intense laser excitation, biexcitons rapidly localize into the band-tail states. The formation time of localized biexcitons becomes shorter with increasing Al composition. Both the inhomogeneous linewidth and the binding energy of biexcitons increase with the inhomogeneous linewidth of excitons. The biexciton binding energy is enhanced by the restriction of exciton motion to disordered potentials and the dynamics of stable biexcitons determines the optical spectrum in mixed crystals.

DOI: [10.1103/PhysRevB.80.075205](https://doi.org/10.1103/PhysRevB.80.075205)

PACS number(s): 78.47.Cd, 71.35.-y, 78.55.Cr

I. INTRODUCTION

In photoexcited semiconductors, an attractive Coulomb interaction between conduction-band electrons and valence-band holes causes excitons to form. The formation of molecules composed of two excitons also becomes possible in a dense exciton system under intense photoexcitation at low temperatures.^{1,2} These are called biexcitons or excitonic molecules. Since the existence of biexcitons was first argued in 1958,³ extensive studies have examined their optics in semiconductors.^{1,2} Biexcitons play an essential role in the optical responses of wide band gap semiconductors and semiconductor nanostructures because of their large exciton binding energies and strong electron-hole correlations. In semiconductor mixed crystals and nanostructures, the localization of biexcitons occurs in random-potential fluctuations induced by compositional fluctuations in mixed crystals or by interface roughness in nanostructures.⁴⁻⁸ Although biexciton and exciton localization are crucial for stimulated emission and optical gain processes in highly excited mixed crystals and nanostructures,⁹⁻¹² the dynamical behavior of localized biexcitons is still unclear compared to that of localized excitons.¹³⁻¹⁸

Random potential fluctuations in mixed crystals, or alloy disorders, strongly affect the photoluminescence (PL) dynamics of excitons. Disorder-induced localization of excitons is observed as line broadening in optical transitions around the band edge. Because a biexciton is a composite of two excitons (two electrons and two holes), both attractive Coulomb interaction between electrons and holes and repulsive Coulomb interaction between two electrons (or holes) are enhanced due to the spatial localization. Thus, the optical spectrum and dynamics of biexcitons in mixed crystals are complicated. A satisfactory and systematic analysis of biexcitons in mixed crystals has so far not been performed. Due to the very small exciton Bohr radii in wide-gap GaN-based mixed crystals, their optical properties are very sensitive to spatial potential fluctuations.¹⁹⁻²² $\text{Al}_x\text{Ga}_{1-x}\text{N}$ mixed crystals are therefore well suited for the study of biexciton dynamics in semiconductor mixed crystals.

In this paper, we report subpicosecond time-resolved PL spectra of biexcitons in highly excited $\text{Al}_x\text{Ga}_{1-x}\text{N}$ mixed

crystals at low temperatures as a function of the Al composition. We observe that under an exciton resonant excitation, the biexciton localization becomes more rapid with increasing Al composition, and that the PL linewidth and the survival time of free biexcitons depend on the composition of the sample. Moreover, the composition-dependent biexciton PL dynamics reflects the biexciton binding energy which is enhanced by the restriction of exciton motion in disordered potentials.

II. EXPERIMENTAL

The samples were $\text{Al}_x\text{Ga}_{1-x}\text{N}$ and GaN epitaxial films. Following the deposition of 1- μm -thick GaN buffer layers, 1- μm -thick $\text{Al}_x\text{Ga}_{1-x}\text{N}$ epitaxial layers were grown on (0001) sapphire substrates using a metalorganic chemical vapor deposition technique.²³ The $\text{Al}_x\text{Ga}_{1-x}\text{N}$ epitaxial layers used in this study had Al concentrations of $x=0.019$, 0.038, 0.057, and 0.077. Wavelength-tunable femtosecond laser pulses, obtained from an optical parametric amplifier system based on a regenerative amplified Ti:sapphire laser, were used as the excitation source. The pulse duration and repetition rate were ~ 150 fs and 1 kHz, respectively. The sample temperature was kept at 7 K, and the typical laser spot size on the samples was 100 μm . An optical Kerr gate method in a 1-mm-thick quartz cell with toluene as the Kerr medium was used for the time-resolved PL spectral measurements, with a time resolution of 0.7 ps. The PL spectra were measured as a function of delay time using a liquid-nitrogen-cooled charge-coupled device (CCD) with a 50-cm single monochromator.

III. RESULTS AND DISCUSSION

Figures 1(a)–1(c) show the time-resolved PL spectra of $\text{Al}_x\text{Ga}_{1-x}\text{N}$ ($x=0.019$, 0.038, and 0.077) under 0.5 mJ/cm^2 excitation. The excitation energy was set at the free exciton energy for each sample. At a few picoseconds delay, a broad PL spectrum clearly appears in all the $\text{Al}_x\text{Ga}_{1-x}\text{N}$ ($x=0.019$, 0.038, 0.057, and 0.077) samples. The PL dynamics in different samples are similar to each other, and the PL spectra show asymmetrical shapes with lower energy tails. Two-

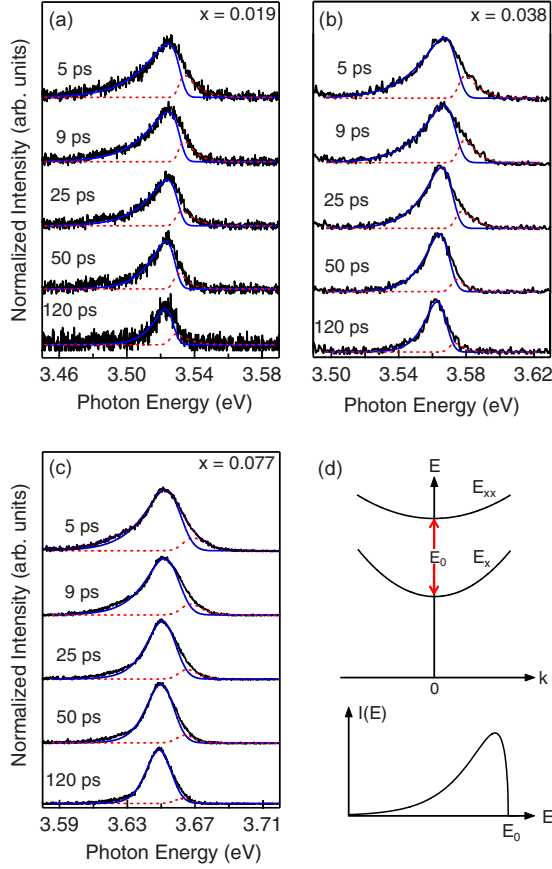


FIG. 1. (Color online) Time-resolved PL spectra measured under exciton resonant excitation in $\text{Al}_x\text{Ga}_{1-x}\text{N}$ mixed crystals: (a) $x=0.019$, (b) $x=0.038$, and (c) $x=0.077$. Solid and broken curves show the fitting results of biexcitons using Eq. (1) and excitons, respectively. (d) Schematic illustration of the energy diagram for exciton (E_x) and biexciton (E_{xx}) (upper figure), and the spectrum shape of the biexciton PL (lower figure).

photon absorption experiments also showed that the PL band has a lower energy tail. This asymmetrical PL band is due to biexcitons.^{7,8} With time evolution, the spectra begin to redshift and narrow, and biexcitons are localized into the lower-energy band-tail state. After about a 100 ps delay, the emission-peak energy becomes independent of time and the spectral shape becomes symmetrical, indicating the relaxation of biexcitons into the lowest band-tail states.

In Figs. 1(a)–1(c), at the early time delays, the spectral shape has a higher energy tail, fitting the Maxwell-Boltzmann distribution for free excitons.⁸ To examine biexciton dynamics separately from that of excitons, we decomposed the PL spectrum into the exciton and biexciton components. It is known that free-biexciton PL spectra in binary semiconductors are well fitted by the inverse Maxwell-Boltzmann distribution function with Lorentzian broadening, while free-exciton PL spectra by the Maxwell-Boltzmann distribution function with Lorentzian broadening.¹ In mixed crystals, however, variations of the binding energy and localization energy of biexcitons lead to spectral broadening due to alloy disorders. In the biexciton spectral analysis in mixed crystals, inhomogeneous broadening needs to be taken into account by convolution of the inverse Maxwell-

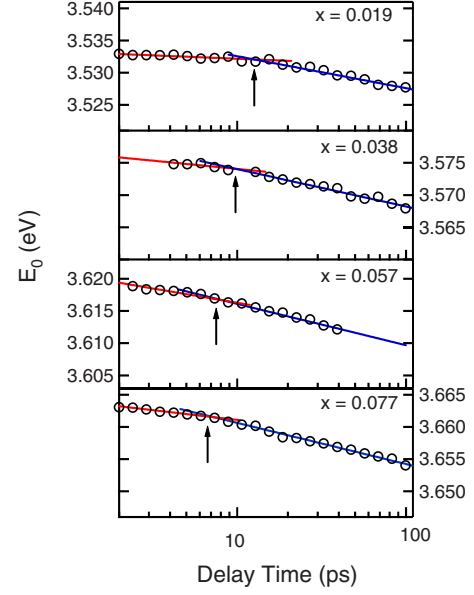


FIG. 2. (Color online) Temporal evolution of the edge energy E_0 in the $\text{Al}_x\text{Ga}_{1-x}\text{N}$ with $x=0.019$, 0.038 , 0.057 , and 0.077 . The solid lines are visual guides.

Boltzmann distribution function with a Gaussian function,

$$I(\hbar\omega_m) \propto \int [E_0 - \varepsilon]^{1/2} \exp[-(E_0 - \varepsilon)/k_B T_e] \times \exp\left[-\left(\frac{\hbar\omega_m - \varepsilon}{\Gamma}\right)^2 \ln 2\right] d\varepsilon, \quad (1)$$

where E_0 is the edge energy of the biexciton PL, corresponding to the energy difference between the lowest-energy biexciton and exciton at a given delay time, as illustrated in Fig. 1(d), and T_e is the effective temperature of biexcitons.⁸ Γ is an inhomogeneous broadening parameter determined from time-integrated PL spectra in Refs. 7 and 8, and it depends on the composition x in mixed crystals. We use Eq. (1) with inhomogeneous broadening included to analyze and discuss the essential features of the biexciton PL spectra, as shown by the solid lines in Figs. 1(a)–1(c). The PL biexciton spectral shapes are well reproduced by the above equation. We obtain the edge energy of the biexciton PL E_0 from the biexciton spectral fitting of the time-resolved PL spectra. In a previous paper,⁸ we demonstrated that the edge energy E_0 is a good indicator of the localization of biexcitons. The edge energy E_0 in mixed crystals is time-dependent because the mixed crystals have band-tail states. Note that the observed PL spectra can be fitted by the inverse Maxwell-Boltzmann model including the shift of the edge energy, rather than by Gaussian spectral shapes. This fact means that at early time delays the spectral shape of localized biexcitons is dominated by the homogeneous broadening due to high T_e rather than inhomogeneous Γ . In this case, biexcitons are weakly localized in shallow localized states and the redshift of edge energy E_0 indicate the appearance of localization.

Figure 2 shows the temporal evolution of the edge energies of biexciton PL in all samples. The edge energy E_0

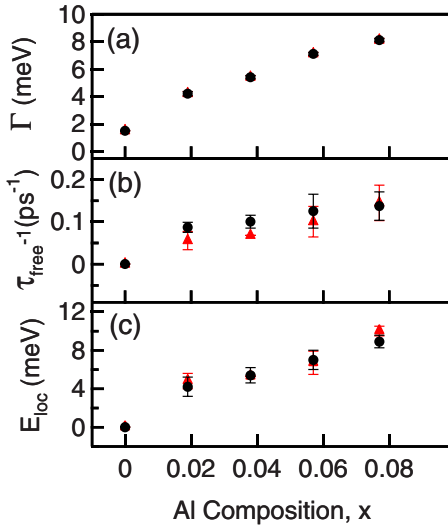


FIG. 3. (Color online) Al composition dependence of (a) the biexciton PL line broadening, Γ , (b) the formation rate of biexcitons, τ_{free}^{-1} , and (c) the localization energy, E_{loc} , obtained by using the Gaussian broadening (circles) and the Lorentzian broadening (triangles).

remains almost constant for delay times of less than a few tens of picoseconds. After a few tens of picoseconds time delay, however, the edge energy E_0 becomes strongly time-dependent. This behavior was completely different from that of the free biexcitons in GaN.⁸ The clear redshift of E_0 in $\text{Al}_x\text{Ga}_{1-x}\text{N}$ mixed crystals suggests that localized biexcitons appear in the band-tail states. The crossing point between free and localized biexcitons, as shown by arrows, indicates the beginning of biexciton localization. The delay time and energy at this crossing point means the survival time of free biexcitons τ_{free} and the edge energy of free biexciton PL E_0^{free} . The survival time τ_{free} decreases as the Al concentration increases.

In Fig. 3(a), we show the broadening parameter Γ (half width at half maximum) as a function of the Al composition. Because the broadening parameter Γ reflects inhomogeneous broadening, the alloy disorder increases monotonically with the Al composition in $\text{Al}_x\text{Ga}_{1-x}\text{N}$ mixed crystals. At the delay time τ_{free} , the localization of biexcitons begins. Then, we define τ_{free}^{-1} as the formation rate of localized biexcitons. In Fig. 3(b), the formation rate of localized biexcitons increases with the Al composition in mixed crystals. This means that the transformation rate from free to localized biexcitons increases because of the alloy disorder scattering.

The time-dependent E_0 of the localized biexcitons ($> \tau_{\text{free}}$) corresponds to the position of averaged biexcitons in the band-tail state. At a delay time of approximately 100 ps, the PL peak energies are almost equal to the peak energies of the time-integrated PL spectra in all samples. This implies that at around 100 ps, the biexcitons are localized at the bottom of the band-tail states. Then, we define the localization energy E_{loc} as the energy difference between E_0^{free} and E_0 at 100 ps, indicating the energy width of the band-tail states for biexcitons. In Fig. 3(c), the localization energy is plotted as a function of the Al composition. It increases with the Al composition.

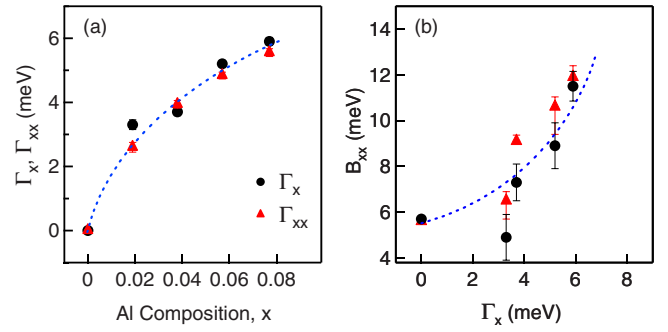


FIG. 4. (Color online) (a) Inhomogeneous linewidths of biexcitons Γ_{XX} and excitons Γ_X as a function of the Al composition. (b) Biexciton binding energy, obtained by using the Gaussian broadening (circles) and the Lorentzian broadening (triangles), as a function of the exciton inhomogeneous line broadening, Γ_X . The broken curves are visual guides.

All these parameters for free and localized biexcitons in Fig. 3 (the inhomogeneous broadening Γ the formation rate of localized biexcitons τ_{free}^{-1} , and the localization energy E_{loc}) increase approximately proportionally to the Al compositions in the Ga-rich $\text{Al}_x\text{Ga}_{1-x}\text{N}$ mixed crystals. This indicates that the alloy disorders enhance the localization of biexcitons in mixed crystals. For comparison, the parameters obtained by using the Lorentzian broadening function as in Ref. 8, are also plotted in Fig. 3. The essential features of the dynamics of the biexciton localization are almost independent of the broadening models (Gaussian or Lorentzian broadening), because high-biexciton temperature broadening is larger than these inhomogeneous one.

We now discuss the biexciton localization process in mixed crystals. Because the radiative annihilation of biexcitons is caused by the transition from biexcitons to free excitons, the observed inhomogeneous linewidth Γ in Fig. 3(a) is determined by both the inhomogeneous linewidths of biexcitons (Γ_{XX}) and excitons (Γ_X): $\Gamma^2 = \Gamma_X^2 + \Gamma_{XX}^2$. Figure 4(a) shows the composition dependence of Γ_{XX} and Γ_X , where Γ_X is deduced from exciton PL spectra. Both Γ_{XX} and Γ_X increase with the Al composition, and the values of Γ_{XX} are almost the same as those of Γ_X in all samples. In addition, the biexciton binding energy B_{xx} is plotted as a function of Γ_X in Fig. 4(b). The biexciton binding energy, corresponding to the energy difference between the free biexciton and twice the free excitons, is evaluated from the energy difference between E_0^{free} and the free exciton energy determined from PL excitation spectra in Ref. 7. The biexciton binding energy increases with the inhomogeneous broadening due to alloy disorders. The biexciton properties Γ_{XX} and B_{xx} are closely correlated with the exciton linewidth in disordered potentials, Γ_X . The enhancement of the biexciton binding energy cannot be explained by an increase of the band gap energy: The biexciton binding energies are 5.7 meV for GaN (Ref. 24) and 19 meV for AlN.²⁵ Based on a linear interpolation of B_{XX} between GaN and AlN crystals, we evaluated that the free biexciton binding energy at the $x=0.077$ sample is 6.7 meV. However, the experimental result of $B_{xx}=11.5$ meV at $x=0.077$ is much larger than the calculated value. This difference indicates that the enhancement of the biexciton bind-

ing energy is caused by the biexciton localization, as discussed below.

In Ga-rich $\text{Al}_x\text{Ga}_{1-x}\text{N}$ mixed crystals, the binding energies of biexcitons B_{XX} are comparable to or larger than both the inhomogeneous broadenings of biexcitons Γ_{XX} , and the localization energies of biexcitons E_{loc} . This implies that biexcitons have large binding energies and are stable even in disorder potentials in mixed crystals. They are most likely not decomposed into two excitons during the relaxation process at the bottom of the localized states. Thus, biexcitons are good excitation particles even in disordered potentials in our samples. Although the volume of an exciton is obviously smaller than that of a biexcitons (a composite of two excitons), we found that the inhomogeneous linewidth of biexcitons Γ_{XX} is approximately equal to that of excitons Γ_X . This indicates that the characteristic confinement volume for excitons and biexcitons due to potential fluctuations is much larger than both the biexciton and exciton volumes. Such a spatial confinement leads to the enhancement of the attractive interaction between the excitons and biexciton binding energy.⁶ In contrast, the strong confinement of excitons and biexcitons leads to the reduction of the binding energy due to the repulsive Coulomb interaction between electrons and holes. Therefore, the weakly confinement causes the strong enhancement of the biexciton binding energy.^{5,6} This enhancement mechanism is completely different from that of the strong confined limit in the quantum dots (the enhance-

ment is caused by a change of Coulomb interaction).²⁶ In Ga-rich $\text{Al}_x\text{Ga}_{1-x}\text{N}$ mixed crystals, the dynamical behavior of biexciton localizations is dominated by the restriction of the exciton center of mass motion.

IV. CONCLUSIONS

We reported the composition dependence of the biexciton PL spectra and the disorder dependent transformation dynamics from free to localized biexcitons in Ga-rich $\text{Al}_x\text{Ga}_{1-x}\text{N}$ mixed crystals. With an increase in the Al composition, the biexciton localization occurs more rapidly under the exciton resonant excitation. The localization-enhanced biexciton binding occurs due to the spatial confinement of excitons. Our findings revealed that biexciton dynamics are strongly affected by the spatial confinement of excitons in disordered potentials in GaN-based mixed crystals.

ACKNOWLEDGMENTS

Part of this study at Kyoto University was supported by a Grant-in-Aid for Scientific Research on Innovative Areas "Optical science of dynamically correlated electrons" (Grant No. 20104006) from MEXT, Japan. One of the authors (D.H.) was supported by JSPS (Grant No. 21-1232).

*Corresponding author. kanemitsu@scl.kyoto-u.ac.jp

¹M. Ueda, H. Kanzaki, K. Kobayashi, Y. Toyozawa, and E. Hanamura, *Excitonic Processes in Solids* (Springer, Berlin, 1986).

²C. Klingshirn, *Semiconductor Optics*, 3rd ed. (Springer, Berlin, 2006).

³M. A. Lampert, Phys. Rev. Lett. **1**, 450 (1958).

⁴J. Y. Bigot, A. Daunois, J. Oberlé, and J. C. Merle, Phys. Rev. Lett. **71**, 1820 (1993).

⁵W. Langbein, J. M. Hvam, M. Umlauff, H. Kalt, B. Jobst, and D. Hommel, Phys. Rev. B **55**, R7383 (1997).

⁶W. Langbein and J. M. Hvam, Phys. Rev. B **59**, 15405 (1999).

⁷Y. Yamada, Y. Ueki, K. Nakamura, T. Taguchi, A. Ishibashi, Y. Kawaguchi, and T. Yokogawa, Phys. Rev. B **70**, 195210 (2004).

⁸D. Hirano, T. Tayagaki, Y. Yamada, and Y. Kanemitsu, Phys. Rev. B **77**, 193203 (2008).

⁹J. Ding, H. Jeon, T. Ishihara, M. Hagerott, A. V. Nurmikko, H. Luo, N. Samarth, and J. Furdyna, Phys. Rev. Lett. **69**, 1707 (1992).

¹⁰W. Wegscheider, L. N. Pfeiffer, M. M. Dignam, A. Pinczuk, K. W. West, S. L. McCall, and R. Hull, Phys. Rev. Lett. **71**, 4071 (1993).

¹¹F. Kreller, M. Lowisch, J. Puls, and F. Henneberger, Phys. Rev. Lett. **75**, 2420 (1995).

¹²Y. Hayamizu, M. Yoshita, Y. Takahashi, H. Akiyama, C. Z. Ning, L. N. Pfeiffer, and K. W. West, Phys. Rev. Lett. **99**, 167403 (2007).

¹³E. Cohen and M. D. Sturge, Phys. Rev. B **25**, 3828 (1982).

¹⁴S. Permogorov, A. Rentitskii, S. Verbin, G. O. Müller, P. Flögel,

and M. Nikiforova, Phys. Status Solidi B **113**, 589 (1982).

¹⁵E. F. Schubert, E. O. Göbel, Y. Horikoshi, K. Ploog, and H. J. Queisser, Phys. Rev. B **30**, 813 (1984).

¹⁶G. Noll, U. Siegner, S. G. Shevel, and E. O. Göbel, Phys. Rev. Lett. **64**, 792 (1990).

¹⁷R. Zimmermann, J. Cryst. Growth **101**, 346 (1990).

¹⁸J. Singh, K. K. Bajaj, and S. Chaudhuri, Appl. Phys. Lett. **44**, 805 (1984).

¹⁹K. Kornitzer, T. Ebner, K. Thonke, R. Sauer, C. Kirchner, V. Schwegler, M. Kamp, M. Leszczynski, I. Grzegory, and S. Porowski, Phys. Rev. B **60**, 1471 (1999).

²⁰G. Coli, K. K. Bajaj, J. Li, J. Y. Lin, and H. X. Jiang, Appl. Phys. Lett. **78**, 1829 (2001).

²¹F. S. Cheregi, A. Vinattieri, E. Feltin, D. Simeonov, J. F. Carlin, R. Butté, N. Grandjean, and M. Gurioli, Phys. Rev. B **77**, 125342 (2008).

²²D. Hirano, T. Tayagaki, and Y. Kanemitsu, Phys. Rev. B **77**, 073201 (2008).

²³Y. Yamada, Y. Ueki, K. Nakamura, T. Taguchi, A. Ishibashi, Y. Kawaguchi, and T. Yokogawa, Appl. Phys. Lett. **84**, 2082 (2004).

²⁴R. Zimmermann, A. Euteneuer, J. Möbius, D. Weber, M. R. Hofmann, W. W. Rühle, E. O. Göbel, B. K. Meyer, H. Amano, and I. Akasaki, Phys. Rev. B **56**, R12722 (1997).

²⁵Y. Yamada, K. Choi, S. Shin, H. Murotani, T. Taguchi, N. Okada, and H. Amano, Appl. Phys. Lett. **92**, 131912 (2008).

²⁶Y. Masumoto, S. Okamoto, and S. Katayanagi, Phys. Rev. B **50**, 18658 (1994).